Freeman, B. A., Sissenstein, R., McManus, T. T., Woodward, J. E., Lee, I. M., & Mudd, J. B. (1976) *J. Bacteriol. 125*, 946–954.
Haque, R., Tinsley, I. J., & Scumedding, D. (1972) *J. Biol. Chem. 247*, 157–161.
Hildebrand, J. G., & Law, J. H. (1964) *Biochemistry 3*, 1304–1308.
Huang, C. H. (1978) *Lipids 12*, 348–356.
Lowry, O. H., Rosebrough, J. J., Farr, A. L., & Randall, R. J. (1951) *J. Biol. Chem. 193*, 265–275.
McElhaney, R. N., & Tourtellotte, M. E. (1970) *Biochim. Biophys. Acta 202*, 120–128.
Op den Kamp, J. A. F., Kauerz, M. Th., & Van Deenen, L. L. M. (1972) *J. Bacteriol. 12*, 1090–1098.
Plackett, P., & Rodwell, A. W. (1970) *Biochim. Biophys. Acta 210*, 230–240.
Razin, S. (1978) *Microbiol. Rev. 42*, 414–470.
Razin, S., & Rottem, S. (1976) in *Biochemical Analysis of Membranes* (Maddy, A. H., Ed.) pp 3–26, Chapman and Hall, London.
Razin, S., & Rottem, S. (1978) *Trend Biochem. Sci. 3*, 51–55.
Rottem, S., & Razin, S. (1973) *J. Bacteriol. 113*, 565–571.
Rottem, S., & Greenberg, A. S. (1975) *J. Bacteriol. 121*, 631–639.
Rottem, S., Slutzky, G. M., & Bittman, R. (1978) *Biochemistry 17*, 2723–2726.
Rudel, L. L., & Morris, M. D. (1973) *J. Lipid Res. 14*, 364–366.
Saito, Y., & McElhaney, R. N. (1978) *Biochim. Biophys. Acta 529*, 224–230.
Saito, Y., Silvius, J. R., & McElhaney, R. N. (1977) *Arch. Biochem. Biophys. 182*, 443–454.
Shaw, N. (1968) *Biochim. Biophys. Acta 164*, 435–436.
Smith, P. F. (1979) in *The Mycoplasmas* (Barile, M. F., & Razin, S., Eds.) Vol. 1, pp 231–258, Academic Press, New York.
Van Deenen, L. L. M. (1965) in *Progress in the Chemistry of Fats and Other Lipids* (Hollman, R. T., Ed.) Vol. 8, pp 37–64, Pergamon Press, Oxford.
Van Gent, C. M., Rozeleur, O. J., & Van der Bijl, P. (1973) *J. Chromatogr. 85*, 174–176.
Wagner, H., Hörhammer, L., & Wolff, P. (1961) *Biochem. Z. 334*, 175–184.
Yavin, E., & Zutra, A. (1977) *Anal. Biochem. 80*, 430–437.

Electron Paramagnetic Resonance Analyses of Horseradish Peroxidase in Situ and after Purification†

M. M. Maltempo,* P.-I. Ohlsson, K.-G. Paul, L. Petersson, and A. Ehrenberg

ABSTRACT: We present EPR spectra of freshly harvested horseradish root, partially purified root extract, and pure horseradish peroxidase isoenzymes A2 and C2 at various values of pH, temperature, and power. They exhibit signals in the $g \simeq 6$ and $g \simeq 5$ region, typical of high-spin and *quantum* mixed-spin heme iron, respectively, with a greater proportion of $g \simeq 5$ signal present in the root and root extract samples than is seen in the spectra of most samples of pure A2 and C2 isoenzymes. The addition of hydroquinone to A2 or C2 causes an increase in the *quantum* mixed-spin signal and an accompanying decrease in the high-spin signal. Tests for adhering donor in the purified isoenzymes were negative, implying that the *quantum* mixed-spin signals, $g \simeq 5$, originate from free horseradish peroxidase. The addition of hydrogen peroxide decreases the $g \simeq 5$ and $g \simeq 6$ signals in parallel with each other and the increase in the free radical signal at $g \simeq 2$. pH titration of A2 or C2 results in reversible transitions between various high-spin, *quantum* mixed-spin, and low-spin EPR spectral species. The variation in the relative amounts of *quantum* mixed-spin and high-spin species monitored in different horseradish peroxidase preparations and the response to conditions of donor and pH show that the protein conformation is sensitive to perturbation imposed upon it during and after purification. The implications of *quantum* mixed-spin properties for the peroxidase function of the enzyme are discussed in the context of the model for the iron–ligand configuration inferred from magnetic studies of *quantum* mixed-spin heme proteins.

The magnetic properties of horseradish peroxidase have been analyzed in a number of papers, including EPR studies under various conditions (Morita & Mason, 1965; Blumberg et al., 1968; Douzou & Leterrier, 1970; Tamura & Hori, 1972; Critchlow & Dunford, 1972; Schonbaum, 1973; Aasa et al., 1975; Leigh et al., 1975). Although qualitatively similar, the results on the free enzyme have differed in both spectral details and interpretation. In particular, an EPR absorption at $g \simeq 5$ has varied considerably from one preparation to another. This fact, the uncommon nature of this signal in heme protein EPR spectra, and the observation that the signal is reinforced by aromatic hydrogen donors raised the question whether the $g \simeq 5$ signal is caused by the free HRP[1] itself or by a complex with some substance from the root.

The EPR spectrum of HRP has been interpreted as originating from a thermal or chemical mixture of high- and low-spin forms of HRP (Tamura, 1971; Tamura & Hori,

† From the Department of Biochemistry and Biophysics, University of Pennsylvania, Philadelphia, Pennsylvania 19174, the Department of Chemistry, University of Umeå, S-901 87 Umeå, Sweden, and the Department of Biophysics, Arrhenius Laboratory, University of Stockholm, S-106 91 Stockholm, Sweden. *Received December 6, 1978; revised manuscript received April 4, 1979.* This work was supported by the Swedish Medical Research Council (13X-4267), by the Swedish Natural Science Research Council, and by a National Institutes of Health Postdoctoral Fellowship (1 F22 GM 02068-01 to M.M.M.).

* Present address: Physics Department, Division of Natural and Physical Sciences, University of Colorado at Denver, Denver, CO 80202.

[1] Abbreviations used: HRP, horseradish peroxidase; RZ, A_{402}/A_{280} (Reinheitszahl).

0006-2960/79/0418-2935$01.00/0 © 1979 American Chemical Society

1972). However, the EPR, resonance Raman (Rakshit & Spiro, 1974), and absorption spectra (Schonbaum, 1973) of HRP show definite similarities to the spectra of ferricytochrome c' at physiological pH (Ehrenberg & Kamen, 1965; Maltempo et al., 1974; Strekas & Spiro, 1974; Kitagawa et al., 1977; Horio & Kamen, 1961). The cytochrome c' data strongly support the view that, in some bacterial species of the protein (e.g., from *Chromatium*), the predominate chemical species at pH 7 has a heme–iron configuration corresponding to a *quantum mechanical* mixture of ($S = 3/2$) mid-spin and ($S = 5/2$) high-spin states (Maltempo et al., 1974; Maltempo, 1974). Quantum mixed-spin heme is characterized by intermediate values of paramagnetic susceptibility (typically, $\mu_{eff} = 3.4$–$3.8\ \mu_B$ at 4.2 K, 5.0–$5.2\ \mu_B$ at 300 K), a single EPR spectral species with $g_\perp \simeq 5$ and $g_\parallel = 2$, a single set of resonance Raman marker bands intermediate in position between the corresponding high-spin and low-spin band, and a Mössbauer spectrum in small applied fields consisting of a four-line hyperfine pattern (Moss & Maltempo, 1978); it usually exhibits absorption peaks at about 400, 500, and 630 nm (Maltempo & Moss, 1976). Magnetic circular dichroism data have been published for HRP and cytochrome c' (Kobayashi et al., 1977; Rawlings et al., 1977). However, MCD cannot categorically distinguish between high-spin and quantum mixed-spin species (Rawlings et al., 1977).

In the present paper, we reexamine the magnetic properties of HRP and eventually reinterprete them, in the context of the novel electronic and structural properties of the quantum mixed-spin state.

Experimental Section

Several batches of horseradish peroxidase isoenzymes A2 and C2 were isolated as previously described (Paul & Stigbrand, 1970; Marklund et al., 1974) to give $A_{403}/A_{280} =$ 4.05–4.15 and 3.35–3.45, respectively. The preparations were homogeneous by chromatography, polyacrylamide gel electrophoresis, and isoelectric focusing. To avoid possible effects of traces of ethanol and acetic acid, and to minimize manipulations, one sample of HRP was partially purified from the freshly grated root only by means of ammonium sulfate fractionation. The final preparation contained 33 mg of dry weight and 4.8 mg of HRP/mL. EPR spectra of horseradish root from the Botanical Garden of the University of Pennsylvania were registered within 20 min after harvesting. HRP and root samples were not deaerated before analyzation in the EPR spectrometer.

Bovine liver Cu–Zn superoxide dismutase was a gift from Dr. S. Marklund, University of Umeå, Sweden. H_2O_2 was assayed by oxidation of Fe(II) cytochrome c with HRP as catalyst (Yonetani, 1965) or by titrating Fe(III) HRP C2 to compound I. Reagents were of analytical grade. Donors were purified by appropriate methods when necessary. When HRP was titrated with donor, the light absorption difference spectra HRP + donor vs. donor showed isosbestic points (Paul & Ohlsson, 1978). Citrate (pH 4, 5), phosphate (pH 6, 7, 8, 11), and carbonate (pH 9, 10) as sodium salts and Tris-HCl (pH 8, 9) were used as buffers, all 100 mM unless otherwise stated.

The EPR spectra were scanned in the region 0–4000 G by using a Varian E-4 spectrometer equipped with an Air Products LTD-3-110 cryostat.

Results

Origin of $g \simeq 5$ EPR Signal. EPR spectra from both the root samples and the partially purified root extract (Figures 1 and 2) exhibited signals in the $g \simeq 6$ and $g \simeq 5$ region, with a greater proportion of $g \simeq 5$ signal than is seen in the spectra

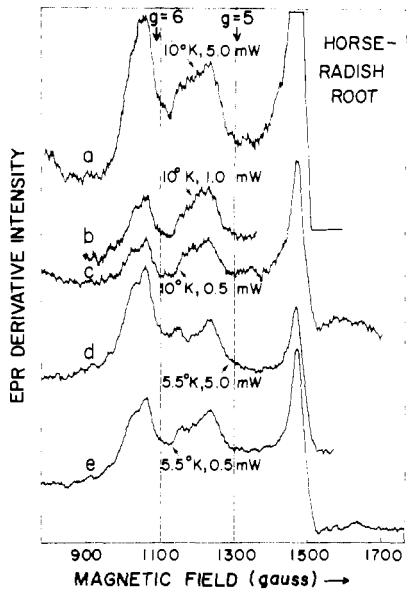

FIGURE 1: EPR spectra of horseradish root, 5.5–10 K, and 0.5–5.0 mW power. Gains (10^{-4}) were 2.0 for traces a–c, 0.4 for d, and 1.0 for e.

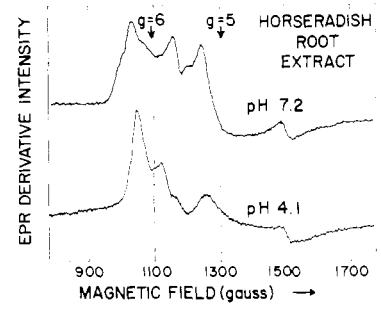

FIGURE 2: EPR spectra of horseradish root extract, at pH 4.1 and pH 7.2, 6 K, and 5.0 mW power.

of most samples of our isolated isoenzymes A2 and C2. There was no evidence of any low-spin Fe(III) heme signals in the region of $g \simeq 3$ (10 K, 1.0 mW). In the root samples, the first signal upfield from $g = 4.3$ was observed at $g = 2.36$; however, this signal had roughly equal peak and trough derivative amplitude, uncharacteristic of the low-field component of typical low-spin ferric heme signals. The different temperature and power dependencies of the signals at $g \simeq 6$ and $g \simeq 5$ (Figure 1) show conclusively that the signals correspond to different electronic transitions. The change in the relative amounts of $g \simeq 6$ and $g \simeq 5$ signals in the root extract upon lowering the pH to 4.1 (Figure 2) is similar to that observed during pH titration of the isoenzymes A2 and C2 (Figures 5 and 6) to acidic pH.

EPR spectra of the two isoenzymes (pH 6) in the field range 775–1800 G, free and in the presence of hydroquinone, are shown in Figure 3. Due to the superposition of high-spin and broader quantum mixed-spin signals in the low-field region, the intensity of the broad trough at 1500 G is the most convenient measure of the quantum mixed-spin signal a_1 of C2 (See Table I). Upon the addition to the isoenzymes of low concentrations of the donor, there is an increase in the $g \simeq 5$ (quantum mixed-spin) signal and an accompanying decrease in the $g \simeq 6$ (high-spin) signal. When added in excess ($\gtrsim 10$ mM) to the C2 isoenzyme, hydroquinone, aniline, resorcinol, and aminotriazole (Figure 3) caused similar spectral transitions. EPR spectra in the temperature range 5–30 K scanning 0–4000 G showed no evidence of an increase in

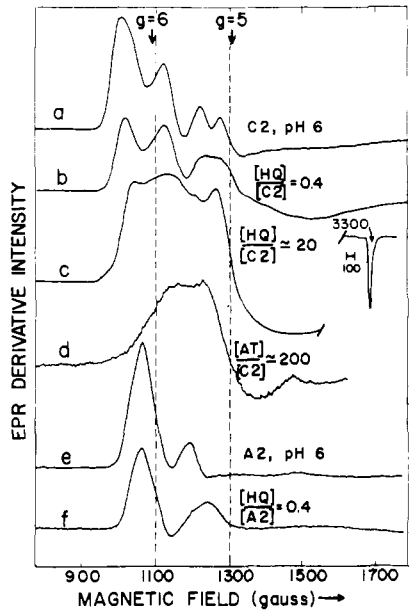

FIGURE 3: EPR spectra of HRP isoenzymes C2 and A2, free and in the presence of hydroquinone (≡ HQ) or aminotriazole (≡ AT). Conditions: a–b were 330 μM HRP, 6 K, 2.0 mW, and 6.3×10^2 gain; c was 665 μM HRP, 6 K, 5.0 mW, and 2.5×10^2 gain; d was 50 μM HRP, 10 K, 5.0 mW, and 2.5×10^3 gain; e–f were 333 μM HRP, 6 K, 2.0 mW, and 10.0×10^2 gain.

Table I: EPR Spectral Species of Horseradish Peroxidase A2 and C2

species	$g_\perp$ values[a]	line width (G)[a]	conditions[b]
A2 a_1	5.0_2	150	pH 9 or hydroquinone bound
a_2	5.6	35	pH 6
b_1	6.2_2, 5.6_8	50	pH 4
b_2	6.4_1, 5.4_4	35	pH 8
b_3	5.8_6	120	pH 5
C2 a_1	5.1	60	pH 6–11
a_2	5.0_2	250	pH 11 or hydroquinone bound
b_1	6.3_4, 5.5_9	40	pH 4
b_2	6.5_9, 5.2	35	pH 8
b_3	6.3, 5.6_9	55	pH 5

[a] The apparent EPR $g_\perp$ values for a rhombic species were taken at the low-field peak and zero-field crossing; the latter field value was used for the $g_\perp$ value for axial signals. In spectra with one or more of the listed spectral species present, a trough at $g = 2.0$ was always observed (see Leigh et al., 1975). The apparent line width of a species was taken as the difference in magnetic field values between a corresponding low-field peak and trough, measured at 5 K. A low-field component of the a_1 species of the C2 isoenzyme, hidden from view below the b_2 low-field peak, cannot be excluded. [b] The pH or donor condition at which one observes the largest amount of a particular spectral species.

low-spin Fe(III) heme signals in the presence of donor.

To test the possibility of an adhering donor, the following experiments were made. (i) Precipitation of pure HRP C2 at pH 6 by means of 6 volumes of ethanol, followed by dialysis, did not change RZ or the proportion of the $g \simeq 5$ signal to the high-spin, $g \simeq 6$ signal. The same result was obtained when an equimolar amount of H_2O_2 was allowed to react with HRP for 10 min at 40 °C before the precipitation. (ii) Splitting of HRP C2 by means of 2-butanone at pH 1.8 and four washings of the apoprotein with 2-butanone, dialysis against bicarbonate, water, and Tris-HCl buffer (in all eight changes), recombination with heme, and chromatography on DEAE-cellulose (Ohlsson & Paul, 1973) caused no significant

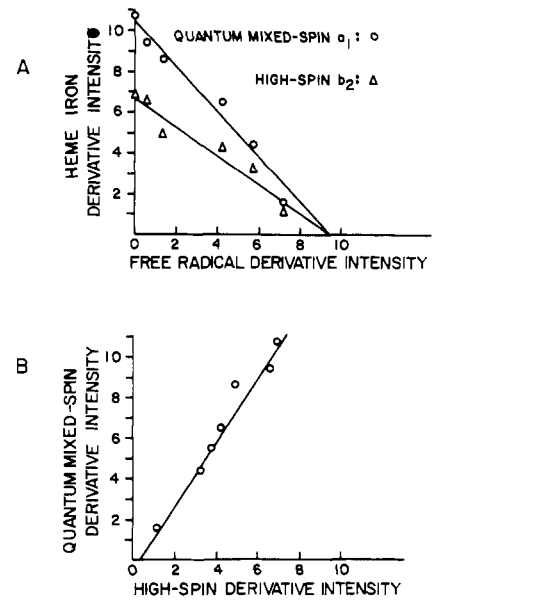

FIGURE 4: (A) A plot of C2 heme iron EPR signals vs. the free radical signal, obtained during titration of HRP with H_2O_2. Spectral species a_1 was quantitated by a peak-to-peak intensity measurement and spectral species b_2 by a peak-to-base line intensity measurement, in the low-field region, at 10 K and 2.0 mW power. The free radical signal was quantitated by a peak-to-peak intensity measurement at $g = 2$, 20 K, and 2.0 mW power. (B) A plot of quantum mixed-spin vs. high-spin EPR derivative intensities obtained during titration of HRP with H_2O_2. Measurements were made as described in A.

change in RZ or the EPR spectrum. (iii) The stepwise addition of H_2O_2 to HRP C2 decreased the $g \simeq 6$ and $g \simeq 5$ signals in parallel with each other and with the increase in the free radical signal at $g \simeq 2$ (Figure 4; see Aasa et al., 1975). (iv) The free radical signals at $g \simeq 2$, seen after the addition of 0.15 and 1.0 H_2O_2 per HRP, showed the same temperature and power dependencies within the accuracy of the experiments (differences < 10%). (v) The addition of superoxide dismutase (up to 25 μg/mL) before or after hydroquinone at pH 6 did not influence the EPR spectrum. From these results, and from the 1:1 combination of added donor and HRP as monitored optically at the Soret band (Paul & Ohlsson, 1978), we conclude that the quantum mixed-spin signal, $g \simeq 5$, originates from the free HRP molecule.

Characterization of EPR Spectral Species. EPR measurements were made by scanning 0–4000 G on the A2 and C2 isoenzymes of horseradish peroxidase under various conditions of pH, temperature, and power to confirm the existence of the individual signal species, as well as in the presence of various donors. Table I summarizes the various high-spin and quantum mixed-spin ($g \simeq 5$) EPR spectral species monitored in the pure C2 and A2 isoenzymes and in the root, along with the corresponding conditions of pH (Figures 5 and 6) and donor (Figure 3). To facilitate the discussion, spectral species with $g_\perp \lesssim 5.6$ are denoted as quantum mixed-spin a type; actually any species with $g_\parallel = 2$ and $4 < g_\perp < 6$ will have some high-spin and mid-spin admixtures. Different temperature and power dependencies of the signals at $g \simeq 6$ and $g \simeq 5$ were observed in purified C2, similar to the results seen in root samples (Figure 1).

Figure 5 shows for the C2 isoenzyme the most frequently occurring performance for the pH dependence of the EPR signal in the pH range 4–11. The observed variability in the relative amounts of the low-field spectral species is consistent with a possible shift of the pH-sensitive range along the pH-scale between different preparations. The cause of these irregularities remains unknown. The spectral transitions were

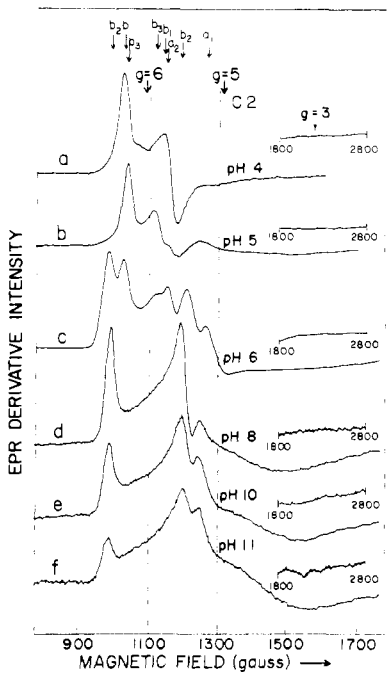

FIGURE 5: EPR spectra of HRP isoenzyme C2, in the pH range 4–11, 775–2800 G, 5 K, and 5.0 mW power. Protein concentration was 50 μM for a, b, d–f and 665 μM for c.

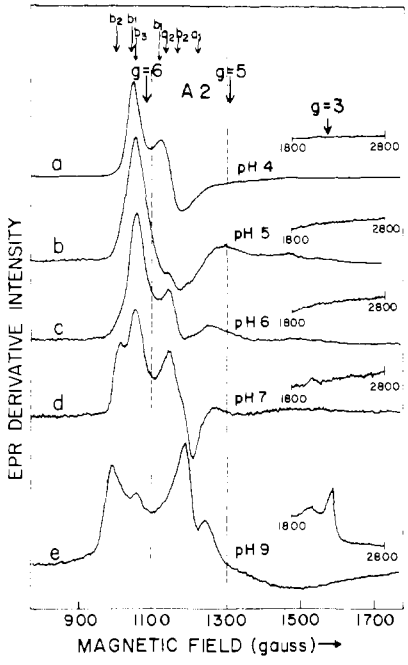

FIGURE 6: EPR spectra of HRP isoenzyme A2, in the pH range 4–9, 775–2800 G, 5 K, and 5.0 mW power. Protein concentration was 50 μM for a–d and 630 μM for e.

reversible in the pH range 4–10. The corresponding EPR spectra for the A2 isoenzyme in the pH range 4–9 are shown in Figure 6. The monitoring conditions in the figure captions provided the best resolution of different spectral species in the region of $g \simeq 5$–6. Small amplitude "trough" signals were observed at $g = 2$, as seen also in previous high-spin and quantum mixed-spin work (Maltempo et al., 1974; Leigh et al., 1975). Peaks at $g = 1.99$ and $g = 1.97$ could unambiguously be assigned to the b_1 and b_2 high-spin species, respectively. The field positions corresponding to the low-field peaks of the various spectral species are labeled in Figures 5 and 6; these peak positions can, of course, be shifted when two or more spectral species overlap.

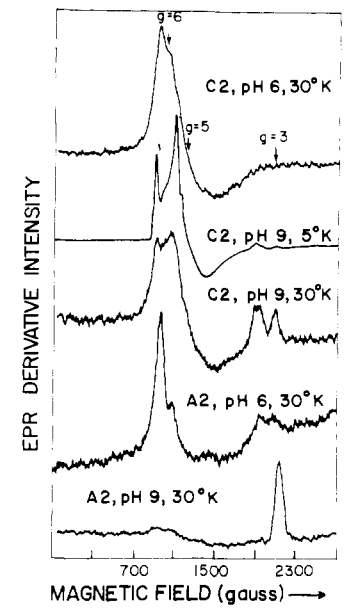

FIGURE 7: EPR spectra of HRP isoenzymes A2 and C2, at pH 6 and 9, 5 K (5 mW) and 30 K (2 mW). Protein concentrations were 630 μM and 665 μM for the A2 and C2 isoenzymes, respectively.

Figure 7 shows the EPR spectra of C2 and A2 at pH 6 and 9, in the temperature range 5–30 K. Different samples were used for the A2 pH 6 spectra in Figures 6 and 7. The C2 pH 9 spectra shown in Figure 7 are somewhat atypical, in that the low-spin signal is stronger than in other samples at that pH. Generally traces of low-spin signals were found when glycine–NaOH or Tris-HCl was used as buffer but not when carbonate was used. The low-spin signals, clearly seen in spectra obtained at 30 K and 2.0 mW, can still be seen at 5 K and 5.0 mW.

Discussion

EPR Spectrum of HRP in Situ. Comparison of the spectra of the intact root and purified HRP indicates an HRP concentration in the root consistent with the value 6 μM deduced from extraction. It is unlikely that a non-peroxidase high- or quantum mixed-spin heme protein could be present in such concentrations and escape detection during the isolation. Heme content and peroxidase activity coincided during chromatography of crude extracts of horseradish root (Shannon et al., 1966). The EPR spectrum of the intact root, the ability of phenolic donor to bind in vitro to isolated HRP A2 and C2, yielding EPR spectra similar to the intact root spectra, and the likely presence of such donors in the root suggest that in vivo HRP may be complexed with donors. It must, however, be left open to what extent the $g \simeq 5$ signal of HRP in situ is due to such donor complexing or to inherent properties of HRP itself.

EPR Spectrum of Pure HRP. The magnetic data presented here and in other publications reveal that free Fe(III) HRP can exist in various high-, low-, and quantum mixed-spin states. The ratio between the high-spin and quantum mixed-spin species can be shifted in either direction by adjusting pH (Figures 5 and 6) or adding a donor. The reversible interconversion of the high-spin and quantum mixed-spin species upon pH titration and the parallel, step-wise reduction of the EPR signal intensity of both spin states upon the addition of H_2O_2 are consistent with the existence of a chemical equilibrium between the two spin states. The addition of phenolic donor (Figure 3) caused a conversion from high-spin species toward quantum mixed-spin species. Benzhydroxamic acid

caused a marked optical and EPR spectral transition (Schonbaum, 1973), which we would interpret as a reverse transition, from quantum mixed spin to high spin. The variation in the relative amounts of quantum mixed spin and high spin monitored in different publications and the response to conditions of donor and pH show that the protein conformation is sensitive to perturbations imposed upon it during and after purification. A definite and reproducible decrease in the $g \simeq 5$ signal and an increase in the $g \simeq 6$ signal appeared even when the A2 and C2 isoenzymes were transferred between an EPR tube and a test tube, without any additions. The relative amounts of the signals were stabilized after 2–4 transfers by means of a pipet. Repeated freezing and thawing in the EPR tube did not affect the EPR spectrum. In a previous publication (Leigh et al., 1975), this effect was incorrectly attributed to the simultaneous addition of donor, but subsequent work has distinguished between this anomalous "handling effect" and donor effects. The former could not be duplicated by the addition of H_2O_2 and was not reversed by heating to 40 °C for 20 min or prevented or abolished by superoxide dismutase. We cannot exclude the possibility that the effect may be due to the exposure to air during transfers, i.e., changes in O_2 or CO_2 content.

Work in progress on the C2 isoenzyme, split and recombined with meso- and diacetyldeuterohemins, indicates a delicate equilibrium between different spin forms also in these cases. The pH dependence for the EPR signal in the low-field region shows generally similar features as in native peroxidase, though the line widths and g values are slightly different. The diacetyldeuterohemin-substituted enzyme shows a significant contribution of low spin, in agreement with the character of its optical spectrum (Ohlsson & Paul, 1973).

The sensitivity of the EPR spectrum to chemical and mechanical perturbation of HRP is consistent with a model, proposed for the quantum mixed-spin state (Maltempo et al., 1974; Maltempo, 1974), in which the heme iron is sensitively poised at an intermediate distance ($d_{\text{low-spin}} < d_{\text{mixed-spin}} < d_{\text{high-spin}}$) out of the porphyrin plane. EPR studies of the HRP–NO complex have identified the fifth ligand as a nitrogen atom (Yonetani et al., 1972 a,b) from histidine (Mauk & Girotti, 1974), which would permit the propagation of contractive strains from the protein moiety to the iron atom. Such strains in domed, but largely high-spin, heme should significantly alter the electrochemical properties of the protein with respect to the propensity of HRP to acquire the Fe(IV) state, a view proposed on the basis of resonance Raman data (Rakshit & Spiro, 1974). It should be noted that recent work has cast some doubt on the traditional view that the magnetic properties of a heme protein are intimately related to the displacement of the iron ion out of the porphyrin plane. A high-spin ferric porphyrin has been reported in which the iron ion is precisely in the plane of an expanded porphyrin core (Mashiko et al., 1978). Two tetramethylene sulfoxide ligands, oxygen bound, serve as weak axial ligands. However, there is no clear crystallographic evidence at present that a high-spin ferric ion with a strong axial ligand may lie in the porphyrin plane. It is appropriate to note that recent resonance Raman studies are in disagreement concerning the amount of iron–porphyrin doming in the resting HRP enzyme, as compared with that of hemoglobin and myoglobin (Felton et al., 1976; Spiro & Burke, 1976).

The increase in the amount of quantum mixed-spin species upon the addition of a phenolic donor should correspond to an increase in the steric strain along the axial iron ligand, and an accompanying increase in the electronegativity of the iron ion. This is in agreement with the observed increase in the dissociation constant of the cyanide and hydroxide complexes of HRP upon the addition of an aromatic donor (Critchlow & Dunford, 1972). Optical and magnetic studies support the view (Chance, 1951) that most donor molecules do not bind directly to the iron (I. Morishima and S. Ogawa, unpublished results; Paul & Ohlsson, 1978), and donor–iron distances in the range of ~6–10 Å have been reported for resorcinol (Leigh et al., 1975), indolepropionic acid (Burns et al., 1975), and *p*-cresol (Schejter et al., 1976).

Magnetic susceptibility data at pH 6.8 showed the paramagnetic moment of free and benzhydroxamic acid bound HRP of type C to be temperature independent between 77 and 250 K, yielding values of 5.97 μ_B for the donor-bound protein and 5.23 μ_B for the free protein (Schonbaum, 1973). The EPR and magnetic susceptibility data indicate that the free HRP sample monitored was essentially all quantum mixed spin (with some high-spin and low-spin components visible by EPR at 4.2 K), and the benzhydroxamic acid bound protein was essentially all high spin. The value of 5.23 μ_B for free HRP is consistent with results from room temperature measurements (Theorell & Ehrenberg, 1952). In another study, the paramagnetic moment of free HRP was temperature dependent between 170 and 270 K, and temperature independent between 90 and 170 K, in the pH range 4.0–9.5 (Tamura, 1971). This was interpreted in terms of a chemical and thermal mixture of high- and low-spin species. However, although the published EPR spectra (Tamura, 1971; Tamura & Hori, 1972) clearly show high- and low-spin species, the absence of an appropriate low-field trough in some of the spectra suggests a significant amount of quantum mixed-spin state.

There is a great similarity between the optical absorption spectra of Fe(III) HRP and Fe(III) cytochrome c'. The spectral transition (350–700 nm) noted upon the addition of benzhydroxamic acid to HRP (Schonbaum, 1973) is of the same type, with respect to change in peak position and intensity, as observed for ferricytochrome c' upon adjusting pH from 7 (quantum mixed spin) to 10 (high spin) (Horio & Kamen, 1961). In both cases, the spectral change observed is consistent with theoretical predictions for a quantum mixed-spin to high-spin spectral transition (Maltempo, 1976).

Thus, magnetic susceptibility and optical absorption data support the EPR evidence that HRP, like ferricytochrome c' (Maltempo, 1975), can exist in various high-, low-, and quantum mixed-spin states, *with an easily perturbed balance between them.*

Chemical Properties and Deduced Heme Configuration. Ferric heme with $g \simeq 5$ (roughly equal mid- and high-spin admixtures) should correspond to a less domed iron–ligand configuration than that typical of high-spin heme; there should be a correlation between the amount of mid-spin admixture and the degree of iron planarity. Figure 8 shows the ordering and population of one-electron d orbitals for heme Fe(III), as well as plots of the corresponding orbital and electrostatic energies for the "fifth" iron 3d electron removed in Fe(III) → Fe(IV) and the "sixth" iron 3d electron added in Fe(III) → Fe(II), as functions of an energy parameter α which provides a measure of the difference in magnitude of the ligand field and electrostatic energy contributions. The iron–ligand configurations on the extreme left and right in Figure 8 correspond to "pure" high-spin and "pure" intermediate-spin states, respectively.

The energy functions plotted in Figure 8 are obtained from a straightforward application of the published analysis of quantum mixed-spin heme states. If E_5 and E_6 denote the

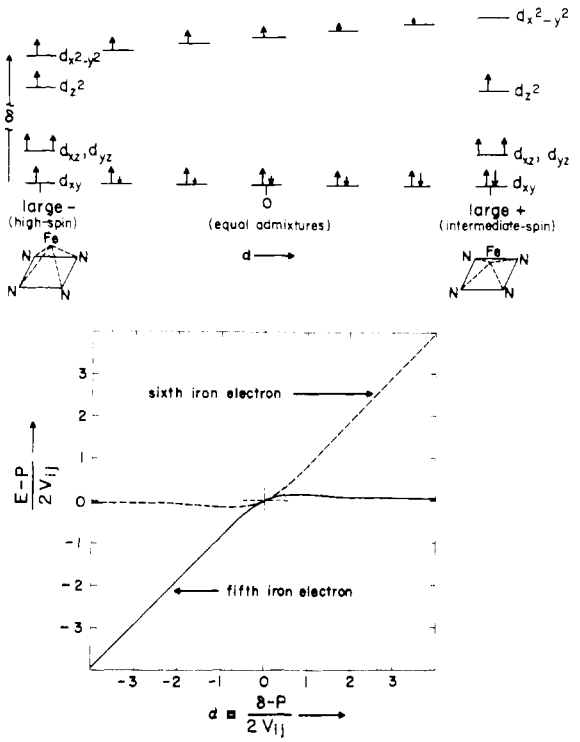

FIGURE 8: The one-electron iron 3d orbitals for heme Fe(III), and the orbital plus electrostatic energies for the "fifth" and "sixth" iron 3d electrons, plotted as a function of the difference between the ligand field and electrostatic energy contributions (see the text for details).

energies of the "fifth" and "sixth" iron 3d electrons, then we obtain eq 1 and eq 2, where δ is the energy difference between

$$E_5 = C_{HS}^2\delta + C_{IS}^2P \quad (1)$$

$$E_6 = C_{IS}^2\delta + C_{HS}^2P \quad (2)$$

the $d_{x^2-y^2}$ and d_{xy} orbitals, P is the electrostatic pairing energy for the two d_{xy} electrons, and C_{HS} and C_{IS} are the high-spin and intermediate-spin coefficients in the ferric mixed-spin wave function, respectively. Substituting in appropriate expressions for C_{HS} and C_{IS}, we obtain eq 3 and eq 4, where $\alpha = (\delta -$

$$\frac{E_5}{2V_{ij}} = \frac{P}{2V_{ij}} + \alpha\left[1 - \frac{1}{2[1 + \alpha^2 - \alpha(1 + \alpha^2)_{abs}^{1/2}]}\right] \quad (3)$$

$$\frac{E_6}{2V_{ij}} = \frac{P}{2V_{ij}} + \frac{\alpha}{2[1 + \alpha^2 - \alpha(1 + \alpha^2)_{abs}^{1/2}]} \quad (4)$$

$P)/2V_{ij}$ and V_{ij} = matrix element for spin–orbit coupling between the $^6A_1$ and $^4A_2$ multiplets. A value $\alpha = 0$ indicates 50% intermediate-spin and 50% high-spin admixtures; increasing positive values of α indicate an increasing amount of intermediate-spin contribution, while more negative values of α indicate an increasing amount of high-spin contribution.

Considerations of the energy associated with different heme–Fe(III) configurations (Figure 8) reveal that it should be easier to remove the fifth iron electron, i.e., go to an Fe(IV) oxidation state, from an Fe(III) state of $\gtrsim$50% intermediate spin admixture ($\alpha \gtrsim 0$) than from an Fe(III) state of essentially high spin. An estimate of the difference in the energy of the fifth iron electron in typical high-spin states and HRP quantum mixed-spin states can be obtained from eq 3. For $V_{ij} = 300$ cm^{-1}, $\alpha = 0$ for a typical $g \simeq 5$ quantum mixed-spin state, and $\alpha = -3$ for a typical $g \simeq 6$ high-spin state (crystal field parameter, D, equal to 10 cm^{-1}), the fifth iron electron would be 223 meV higher in energy in the mixed-spin state than in the typical high-spin state. The redox potential of the Fe(IV)/Fe(III) system in HRP has only been estimated (+1 V, pH 7; George, 1953), and the redox potential of iron-bound H_2O_2 (or OOH) is unknown but may be in the neighborhood of the Fe(IV)/Fe(III) potential. The implication of the quantum mixed-spin conformation would be a shift of the Fe(IV)/Fe(III) redox equilibrium in a direction favorable for the physiological function of HRP (−223 mV in the above example).

Though quantum mixed-spin magnetic properties are certainly not a general prerequisite for peroxidase activity (given the known magnetic and chemical properties of cytochrome *c* peroxidase (Yonetani, 1974)), the ability of the iron to move into the porphyrin plane upon the primary binding of H_2O_2 may indeed be necessary to the peroxidase mechanism. Magnetic susceptibility and Mössbauer studies implicate a low-spin $S = 1$ Fe(IV) state for compound I (as well as compound II) of HRP (Ehrenberg, 1962; Moss et al., 1969; Münck, 1979) and compound ES of cytochrome *c* peroxidase (Iizuka et al., 1968; Lang et al., 1976), consistent with an in-plane position for the heme iron. Resonance Raman data also indicate that the iron ion is in-plane in HRP compound II and cytochrome *c* peroxidase compound ES (Felton et al., 1976). By analogy with the above, this also supports an in-plane iron in HRP compound I.

The energy of the sixth (reducing) electron is strongly α dependent when $\alpha > 0$ but slightly α dependent when $\alpha < 0$ (Figure 8). That is, our model suggests that the Fe(III)/Fe(II) redox potentials for the various high-spin and mixed-spin species are linked to differences not in the energies of the Fe(III) iron acceptor orbitals, but in reduced state heme–protein conformation. It also follows that the two redox systems Fe(IV)/Fe(III) and Fe(III)/Fe(II) would have different dependencies on nonplanarity. Consequently, the Fe(III)/Fe(II) redox system will inform about equatorial and axial substitutions but not about the Fe(IV)/Fe(III) step, involved in the rate-limiting reaction in the peroxidase cycle.

Acknowledgments

The authors thank Drs. B. Chance and T. Yonetani for comments, Dr. G. R. Schonbaum for discussions, and Dr. S. Marklund for a sample of superoxide dismutase. U. B. Mattsson expertly prepared the manuscript. K.-G. Paul expresses his deep gratitude to Dr. Chance for numerous valuable discussions and much generosity during a sabbatical year at the Department of Biochemistry and Biophysics, University of Pennsylvania.

References

Aasa, R., Vänngård, T., & Dunford, H. B. (1975) *Biochim. Biophys. Acta 391*, 259.

Blumberg, W. E., Peisach, J., Wittenberg, B. A., & Wittenberg, J. B. (1968) *J. Biol. Chem. 243*, 1854.

Burns, P. S., Williams, R. J. P., & Wright, P. E. (1975) *J. Chem. Soc., Chem. Commun. 758*, 795.

Chance, B. (1951) *Adv. Enzymol. 12*, 153.

Critchlow, J. E., & Dunford, H. B. (1972) *J. Biol. Chem. 247*, 3714.

Douzou, P., & Leterrier, F. (1970) *Biochim. Biophys. Acta 220*, 338.

Ehrenberg, A. (1962) *Sven. Kem. Tidskr. 74*, 3.

Ehrenberg, A., & Kamen, M. D. (1965) *Biochim. Biophys. Acta 102*, 333.

Felton, R. H., Romans, A. Y., Yu, N., & Schonbaum, G. R. (1976) *Biochim. Biophys. Acta 434*, 82.

George, P. (1953) *Biochem. J. 54*, 267.
Horio, T., & Kamen, M. D. (1961) *Biochim. Biophys. Acta 48*, 266.
Iizuka, T., Kotani, M., & Yonetani, T. (1968) *Biochim. Biophys. Acta 167*, 257.
Kitagawa, T., Ozaki, Y., Kyogoku, Y., & Horio, T. (1977) *Biochim. Biophys. Acta 495*, 1.
Kobayashi, N., Nozawa, T., & Hatano, M. (1977) *Biochim. Biophys. Acta 493*, 340.
Lang, G., Spartalian, K., & Yonetani, T. (1976) *Biochim. Biophys. Acta 451*, 250.
Leigh, J. S., Maltempo, M. M., Ohlsson, P.-I., & Paul, K.-G. (1975) *FEBS Lett. 51*, 304.
Maltempo, M. M. (1974) *J. Chem. Phys. 61*, 2540.
Maltempo, M. M. (1975) *Biochim. Biophys. Acta 379*, 95.
Maltempo, M. M. (1976) *Biochim. Biophys. Acta 434*, 513.
Maltempo, M. M., & Moss, T. H. (1976) *Q. Rev. Biophys. 9*, 181.
Maltempo, M. M., Moss, T. H., & Cusanovich, M. A. (1974) *Biochim. Biophys. Acta 342*, 290.
Marklund, S., Ohlsson, P.-I., Opara, A., & Paul, K.-G (1974) *Biochim. Biophys. Acta 350*, 304.
Mashiko, T., Kastner, M. E., Spartalian, K., Scheidt, W. R., & Reed, C. A. (1978) *J. Am. Chem. Soc. 100*, 6355.
Mauk, M. R., & Girotti, A. W. (1974) *Biochemistry 13*, 1757.
Morita, Y., & Mason, H. S. (1965) *J. Biol. Chem. 240*, 2654.
Moss, T. H., & Maltempo, M. M. (1978) *Bull. Am. Phys. Soc. 23*, 321.
Moss, T. H., Ehrenberg, A., & Bearden, A. J. (1969) *Biochemistry 8*, 4159.
Münck, E. (1979) in *The Porphyrins* (Dolphin, D., Ed.) Academic Press, New York (in press).
Ohlsson, P.-I., & Paul, K.-G. (1973) *Biochim. Biophys. Acta 315*, 293.
Paul, K.-G., & Stigbrand, T. (1970) *Acta Chem. Scand. 24*, 3607.
Paul, K.-G., & Ohlsson, P.-I. (1978) *Acta Chem. Scand., Ser. B 32*, 395.
Rakshit, G., & Spiro, T. G. (1974) *Biochemistry 13*, 5317.
Rawlings, J., Stephens, P. J., Nafie, L. A., & Kamen, M. D. (1977) *Biochemistry 16*, 1725.
Schejter, A., Lanir, A., & Epstein, N. (1976) *Arch. Biochem. Biophys. 174*, 36.
Schonbaum, G. R. (1973) *J. Biol. Chem. 248*, 502.
Shannon, L. M., Kay, E., & Lew, J. Y. (1966) *J. Biol. Chem. 241*, 2166.
Spiro, T. G., & Burke, J. M. (1976) *J. Am. Chem. Soc. 98*, 5482.
Strekas, T. C., & Spiro, T. G. (1974) *Biochim. Biophys. Acta 351*, 237.
Tamura, M. (1971) *Biochim. Biophys. Acta 243*, 249.
Tamura, M., & Hori, H. (1972) *Biochim. Biophys. Acta 284*, 20.
Theorell, H., & Ehrenberg, A. (1952) *Arch. Biochem. Biophys. 41*, 442.
Yonetani, T. (1965) *J. Biol. Chem. 240*, 4509.
Yonetani, T. (1974) in *Microbial Iron Metabolism* (Neilands, J. B., Ed.) p 309, Academic Press, New York.
Yontani, T., Iizuka, T., Asakura, T., Otsuka, J., & Kotani, M. (1972a) *J. Biol. Chem. 247*, 863.
Yonetani, T., Yamamoto, H., Erman, J. E., Leigh, J. S., & Reed, G. H. (1972b) *J. Biol. Chem. 247*, 2447.

Ribonucleotide Reductase from Calf Thymus. Purification and Properties†

Ylva Engström, Staffan Eriksson, Lars Thelander,* and Margareta Åkerman

ABSTRACT: Ribonucleotide reductase from calf thymus was purified 3400-fold in good yield by using a rapid and highly reproducible procedure which included ammonium sulfate fractionation, chromatography on DEAE-cellulose and hydroxylapatite and affinity chromatography on dATP–Sepharose. Nonheme iron is an essential component of the enzyme since EDTA causes inactivation which can be reversed by readdition of iron. Data from polyacrylamide gel electrophoresis, glycerol gradient centrifugation, iron analysis, and kinetic experiments indicated that the enzyme preparation consists of two kinds of polypeptide, both necessary for activity. One polypeptide has a molecular weight of about 84 000 and constitutes the bulk of the protein in the final enzyme preparation, while the other iron-binding polypeptide is present in low, nonstoichiometric amounts. The active enzyme complex has a sedimentation coefficient of 10 S but, on addition of the inhibitory effector dATP, most of the protein sediments more rapidly at 16 S. In this respect, the thymus reductase resembles the *Escherichia coli* ribonucleotide reductase which also forms dATP-induced aggregates. Furthermore, the proposed subunit structure of the thymus enzyme is very similar to the one of the bacterial enzyme, which consists of two kinds of polypeptide, molecular weight 80 000 and 39 000, where the 39 000 polypeptide contains nonheme iron and a free radical. However, the thymus enzyme is inhibited reversibly by hydroxyurea or 2′-deoxy-2′-azidocytidine diphosphate in contrast to the *E. coli* reductase which is inactivated by these reagents. These results suggest the possibility of a different structure or environment for the free radical in the mammalian enzyme.

Deoxyribonucleotides are synthesized by direct reduction of the corresponding ribonucleotides in a reaction catalyzed by ribonucleotide reductase. The level of enzyme activity is correlated to the growth rate of the tissue involved. This observation plus the finding that the pools of deoxyribonucleoside triphosphates in cells are very low indicates that the reaction catalyzed by ribonucleotide reductase plays a critical role in DNA synthesis and cell division (Thelander & Reichard, 1979).

† From the Medical Nobel Institute, Department of Biochemistry I, Karolinska Institute, S-104 01 Stockholm, Sweden. *Received February 16, 1979.* This investigation was supported by grants from the Swedish Natural Science Research Council, Magnus Bergvalls Stiftelse, and the Medical Faculty of the Karolinska Institute.

0006-2960/79/0418-2941$01.00/0 © 1979 American Chemical Society